Trap-enhanced electric fields in semi-insulators: The role of electrical and optical carrier injection

Stephen E. Ralph and D. Grischkowsky
IBM T. J. Watson Research Center, P. O. Box 218, Yorktown Heights, New York 10598

(Received 28 May 1991; accepted for publication 23 July 1991)

We report extremely large field enhancement near the anode of an electrically biased metal/semi-insulator/metal structure. The large anode field results from a trap-enhanced space-charge region and is large enough to cause injection of holes at the anode. Our numerical simulations confirm this interpretation and show that for typical semi-insulating GaAs, large trap-enhanced fields (TEF) are to be expected. The TEF effect, contrary to that observed in doped materials, is enhanced by optical injection of carriers near the anode, and can be exploited for the efficient generation of ultrafast THz radiation.

Recent work involving optical excitation of coplanar transmission lines fabricated on compensated semiconductors (semi-insulators) has shown enhanced electrical signal generation for localized excitation of the positively biased electrode.[1] The electrical pulse was more than ten times larger compared to cathode illumination. Additionally, similar enhancements were observed in the generation of THz radiation.[2] Illumination of the anode resulted in radiation more than 50 times stronger than when illuminating the cathode. The generation of THz radiation is a particularly appropriate probe of the underlying features of the enhancement because the generation relies on the rapid acceleration of mobile charge within an electric field. The field strength is thus central to the efficient production of THz radiation.

Although coplanar transmission lines, as well as other geometries, have been used extensively on semi-insulating materials in the detection of ultrashort optical pulses and in the generation and detection of ultrafast electrical transients, very little work has been reported which specifically evaluates the field distributions of these structures with current injection or under nonuniform optical illumination. In this letter we show that a strong field enhancement at the anode of metal-semi-insulator-metal (M/SI/M) structures is responsible for the polarity and positional dependant enhancements and that these enhancements can be controlled by optical and electrical current injection. We have observed using an 80 μm electrode separation on SI-GaAs, that up to 90% of the applied potential may exist within 5 μm of the anode. We find that a space-charge region, resulting from a change in the trap occupancy, forms near the anode. This trap-enhanced field (TEF) at the M/SI interface results from a number of physical mechanisms including (i) the quasi-static nonlinear field distribution (geometric effects), (ii) electron velocity saturation, (iii) space charge of uncompensated residual acceptors resulting from the increasing occupancy of deep traps, and (iv) field-enhanced carrier injection. We present current-voltage (I-V) data which demonstrate large hole injection which we attribute to barrier height lowering associated with the large anode field. Additionally, we present the results of a two-dimensional numerical analysis which shows extremely large fields, $\sim 10^6$ V/cm, near the anode.

Figure 1 shows the measured THz signal strength as a function of the position of the focused illumination spot (5-μm-diam, 60 fs full width half maximum, $\hbar\omega = 2.0$ eV) between two parallel 10-μm-wide metal fabricated lines on liquid-encapsulated Czochralski-grown SI-GaAs. The experimental arrangement is the same as described in Ref. 2. We attribute the variation in THz emission entirely to a changing electric field strength. The SI character of GaAs results from the intentional doping of carbon which is incorporated as an acceptor, $N_a \sim 10^{15}$ cm^{-3}. These acceptors are compensated via deep traps in the form of the EL2 defect at a concentration of $N_t \sim 10^{16}$ cm^{-3}. The contact metallization is annealed AuGeNi characterized by a barrier height ϕ_b which we have measured to be <0.6 eV. Anode enhancement of the THz signal has been observed in all of our SI-GaAs samples including samples which were not annealed, and structures with various line separations. The radiated THz signal is also strongly dependent on bias voltage, exhibiting a dramatic increase in strength at a threshold of ~ 15 V for an 80 μm line separation. These observations, both the apparent large asymmetry in field distribution and the threshold like behavior, are explained by considering the current transport characteristics of the structures.

Figure 2 shows the I-V characteristics for three coplanar structures without illumination. The previously observed THz signal strength versus voltage on an 80 μm structure is also shown.[2] In general, four regions of current transport behavior occur. These regimes are most distinct with an 80 μm line separation but exist to a lesser degree with 50 and 120 μm separations. The different transport regimes, labeled R1–R4 for the 80 μm structure, are R1, a purely linear response at low bias indicating ohmic conduction governed by the high bulk resistivity; R2, a V^2 current dependance resulting from space-charge limited (SCL) electron flow;[3,4] R3, a decreasing current associated with negative differential electron velocity; and R4, a double injection current indicated by a V^3 response. The *transition* to this regime is associated with a sharply increasing THz signal.

Some conclusions are immediately obvious. First, non-

 0003-6951/91/411972-03$02.00

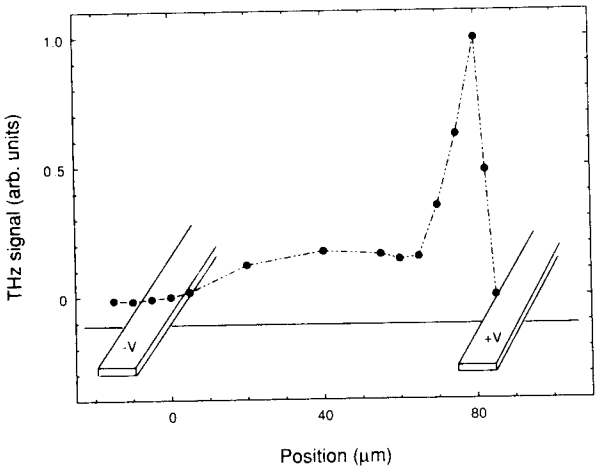

FIG. 1. Measured THz signal as a function of illumination position for an electrode bias of 67 V.

linear transport begins at very low voltages ~4 V, corresponding to average field strengths of 500 V/cm. Second, for negative differential velocity to appreciably affect the net current, the majority of the volume surrounding at least one contact must sustain a field of greater than 4 kV/cm, the field of peak electron velocity, and the spreading resistance at the contacts must be comparable to the bulk resistance between the electrodes. Using conformal mapping techniques[5] we have determined that geometric effects alone are sufficient to cause velocity saturation at low bias and that the spreading resistance is a large fraction of the total resistance. Consequently, the fields near the edge of the electrodes are much greater than 4 kV/cm for biases of 4V.

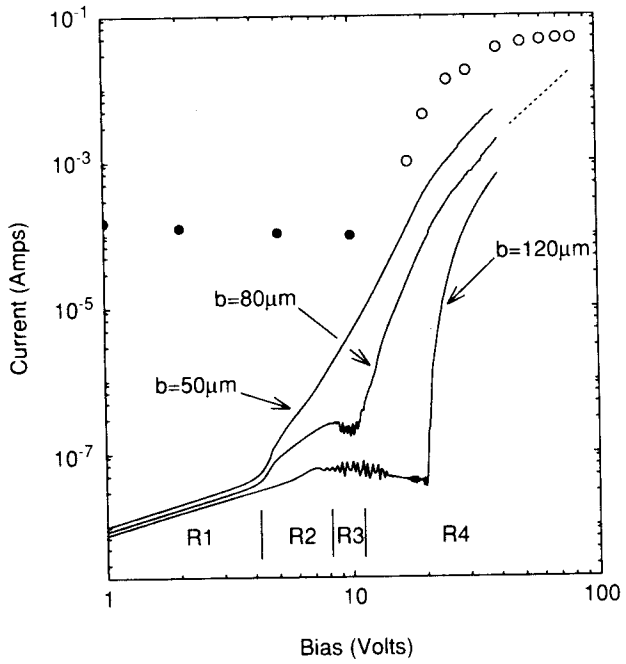

FIG. 2. Current-voltage characteristics (solid lines) for three coplanar electrode separations $b = 50$, 80, and 120 μm. The observed THz signal amplitude (from Ref. 2) for edge illumination is also indicated for an 80 μm structure (open circles and filled circles are of opposite sign). For the high bias regime R4, the current varies as V^3 indicating a double injection process, the dashed line indicates a V^3 response.

The V^3 current response of regime R4 is a unique characteristic of double injection current transport.[5] Thus the sudden increase in both electrode current and THz emission is associated with the injection of holes at the anode. Therefore, the field at the interface E_m, is also large enough to produce significant hole injection via field-induced barrier lowering or tunneling. Note that hole injection is not necessary for the existence of the enhanced anode field nor enhanced THz emission. The effective barrier height lowering can be expressed as[6,7]

$$\Delta\phi = \phi_b - \sqrt{qE_m/4\pi\epsilon_s} - \alpha E_m, \tag{1}$$

where ϵ_s is the static permittivity and α is of the order 40 Å.[7] In GaAs, field strengths of nearly 10^6 V/cm are necessary to produce an effective barrier height lowering of 300 meV which is needed to allow the hole current densities observed.

The field required by (1) cannot be explained by geometric effects alone. It is necessary to consider current transport in the presence of traps. The charge state of the EL2 defect, which has a larger capture cross section for electrons than for holes, is strongly affected by the density of free electrons and holes. The region near the forward biased positive contact experiences an accumulation of electrons and a depletion of holes which is strongly enhanced by electron velocity saturation and geometric effects. The change in the free-carrier densities together with the different capture cross sections combine to dramatically alter the fixed space charge. Although the free-carrier density is not sufficient to cause significant field perturbation via the Poisson equation directly, it has been shown[8,9] using the Shockley–Read–Hall trap description that small changes in free-carrier density result in a large change in trap occupancy. A small-signal analysis shows that the Poisson equation can be written

$$\rho = q\alpha_p(p - p_0) - q\alpha_n(n - n_0), \tag{2}$$

where q is the electron charge, n and n_0 are the nonequilibrium and equilibrium electron densities, respectively (correspondingly, p and p_0 for holes), α_n and α_p are amplification factors given by

$$\alpha_n = \frac{N_t\tau_p r^2(1-r)}{n_0\tau_p r + p_0\tau_n(1-r)},$$

$$\alpha_p = \frac{N_t\tau_n r(1-r)^2}{n_0\tau_p r + p_0\tau_n(1-r)}. \tag{3}$$

N_t is the trap density; τ_p and τ_n are the electron and hole capture lifetimes, respectively, and r is the compensation ratio N_a/N_t. Typical values for α_n and α_p are 5×10^7 and 3×10^6. Thus, electron densities greater than the equilibrium value n_0 result in a substantially larger net negative charge density. Simply, the increased electron density results in larger electron occupancy of the EL2 trap which had been responsible for compensation of the net residual acceptors. The uncompensated ionized acceptors result in a space-charge region which is limited only by the net acceptor concentration. The cathode, on the other hand, experiences only a small electron depletion since the barrier is

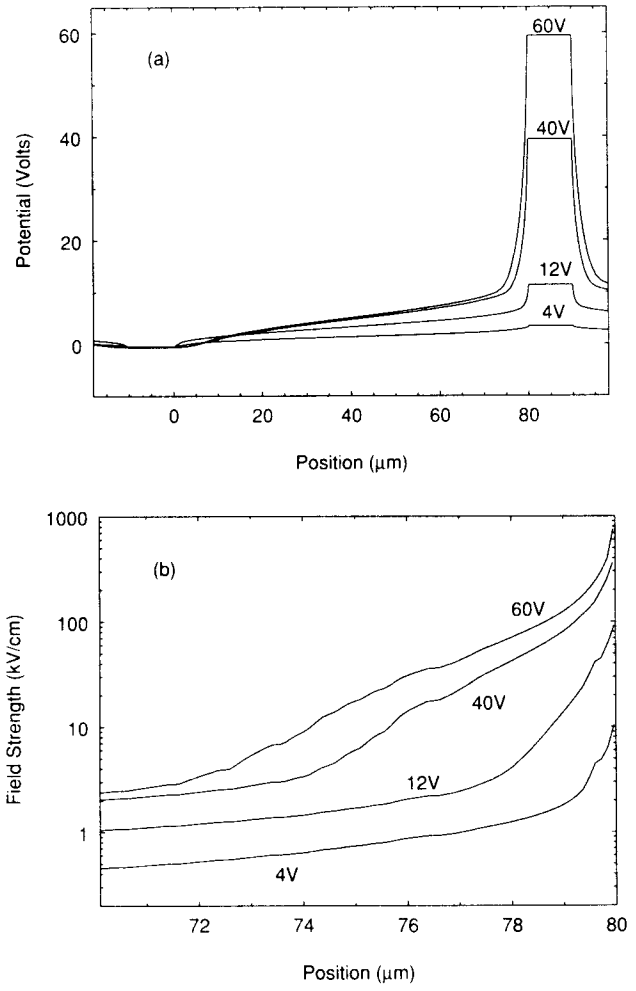

FIG. 3. Results of the two-dimensional numerical simulation of 80 μm structures. The SI-GaAs is characterized by $N_t = 1.5\times10^{16}$ cm^{-3}, $N_a = 1\times10^{15}$ cm^{-3}, $E_t = 0.68$ eV (trap energy measured from the conduction band), $\phi_b = 0.5$ eV, $\tau_n = 5$ ns, and $\tau_p = 6$ μs, (a) potential distribution, (b) electric field near the anode.

sufficiently low and electrons are readily injected. Additionally, the hole velocity saturates at larger fields than electrons and without experiencing a negative differential velocity regime. Thus, the accumulation of holes near the cathode is small and significant fixed space charge does not form.

This interpretation is confirmed by the results of a two-dimensional numerical simulation. Figure 3 depicts the potential distributions and fields near the anode for three of the current transport regimes identified in Fig. 2. For the simulations we have used typical material parameters, although we have found that the general features of the potential profiles do not change appreciably for material that has $N_a > 1\times10^{14}$, $r < 0.1$, and $\phi_b < 0.6$ eV. For low bias the potential distributions are the same as the conformal mapping result. At intermediate and higher voltages the potential distribution is calculated allowing for enhanced injection, $\Delta\phi_b = 200$ meV. The electric fields corresponding to 60 V bias show that the field approaches 10^6 V/cm at the metal-SI interface with fields greater than 3×10^4 extending nearly 4 μm from the interface. These large fields at the anode are responsible for the enhanced electrical and THz signal generation and thereby explain the results of Fig. 1.

Further evidence of the strength of this effect is seen by monitoring the substrate potential and surface potentials between the electrodes. We have observed a clamping effect at the threshold voltage in which the midpoint potential between electrodes becomes clamped to a fixed potential with respect to the cathode. Thus, applied potentials beyond the threshold value appear predominantly near the anode.

The effect of optical injection of carriers has also been investigated. If the structure is biased well into the double injection regime, the optical response is determined by the established local field. Thus, carriers photoexcited within the high-field region near the anode produce a dramatic field-enhanced THz response.

When the structure is biased below the threshold voltage, illumination can have an appreciable effect on the potential distribution. By monitoring the I-V characteristic as a function of illumination position of the femtosecond source, we have verified that optical injection of carriers does force the structure into the double injection regime at voltages lower than without localized illumination. This "optical biasing" is most effective when carriers are locally injected near the anode. This is understood as a reduction of the space charge of the electron current (regime R2) by the optically injected holes which are swept across the structure. Clearly, the larger the region traversed by the holes and the less by the electrons, the greater the space-charge reduction. We have estimated the hole transit time to be of the order 30 ns compared to the pulse period of 10 ns. Suggesting that ample hole current and therefore field enhancement remains for the next pulse. Transient photocurrent measurements confirm this behavior.

In summary, we have presented both experimental results and numerical simulation which establishes the existence of extremely large fields near a positively biased metal SI-GaAs interface. These large trap-enhanced fields are easily produced, may be enhanced by optical injection and therefore may be more common than is currently realized.

We thank Nir Katzenellenbogen and Alan Warren for illuminating discussions and D. J. Frank for assistance with the numerical simulation.

[1] D. Krökel, D. Grischkowsky, and M. B. Ketchen, Appl. Phys. Lett. **54**, 1046 (1989).
[2] N. Katzenellenbogen and D. Grischkowsky, Appl. Phys. Lett. **58**, 222 (1991).
[3] M. A. Lampert and P. Mark, *Current Injection in Solids* (Academic, New York, 1970).
[4] H. J. Queisser, H. C. Casey, and W. van Roosbroeck, Phys. Rev. Lett. **26**, 551 (1971).
[5] C. P. Wen, IEEE Trans. Microwave Theory Tech. **MTT-17**, 1087 (1969).
[6] S. M. Sze, *Physics of Semiconductor Devices* (Wiley, New York, 1981).
[7] J. M. Shannon, Solid-State Electron **19**, 537 (1976).
[8] J.-C. Manifacier and H. K. Henisch, Phys. Rev. B **17**, 2648 (1978).
[9] P. M. Solomon and K. Weiser (unpublished).